

Cyclodextrin metal-organic framework as vaccine adjuvants enhances immune responses

Congcong Li^{a*}, Chaoxi Chen^{a,b*}, Yucai Wei^a, Min Tan^a, Shuo Zhai^a, Juebo Zhao^a, Lu Wang^{a,b} and Tao Dai^c 

^aCollege of Animal & Veterinary Sciences, Southwest Minzu University, Chengdu, China; ^bKey Laboratory of Qinghai-Tibetan Plateau Animal Genetic Resource Reservation and Utilization, Chengdu, China; ^cCollege of Chemistry & Environment, Southwest Minzu University, Chengdu, China

ABSTRACT

It is urgently needed to develop novel adjuvants for improving the safety and efficacy of vaccines. Metal-organic frameworks (MOFs), with high surface area, play an important role in drug delivery. With perfect biocompatibility and green preparation process, the γ -cyclodextrin metal-organic framework (γ -CD-MOF) fabricated with cyclodextrin and potassium suitable for antigen delivery. In this study, we modified γ -CD-MOF with span-85 to fabricate the SP- γ -CD-MOF as animal vaccine adjuvants. The ovalbumin (OVA) as the model antigen was encapsulated into particles to investigate the immune response. SP- γ -CD-MOF displayed excellent biocompatibility *in vitro* and *in vivo*. After immunization, SP- γ -CD-MOF loaded with OVA could induce high antigen-specific IgG titers and cytokine secretion. Meanwhile, SP- γ -CD-MOF also significantly improved the proliferation of spleen cells and activated and matured the bone marrow dendritic cells (BMDCs). The study showed the potential of SP- γ -CD-MOF in vaccine adjuvants and provided a novel idea for the development of vaccine adjuvants.

ARTICLE HISTORY

Received 14 September 2021
Revised 19 November 2021
Accepted 22 November 2021

KEYWORDS

γ -cyclodextrin metal-organic framework; vaccine adjuvants; immune responses

1. Introduction

Vaccination is effective and powerful in preventing and treating infections. Compared with the traditional inactivated and attenuated vaccines, protein antigen-based vaccines have better safety and lower cost, but protein antigens are easy to degrade, with poor immunogens when administered alone (Bobbala & Hook, 2016). Therefore, the application of antigen-based vaccines in biomedicine is limited. Thus, it is essential to use the delivery vehicle and adjuvant to improve immune response (Baldwin et al., 2008; Zhao et al., 2020). Freund's complete adjuvant (FCA), the most common adjuvants, has been extensively used in animal vaccines because of its particular strong stimulant to both cellular and humoral immunities (Li et al., 2019). However, FCA can cause serious adverse reactions, including persistent pain, local tissue necrosis, and tumor-like hyperplasia at the injection site (Lukacs et al., 2015; Nakamura et al., 2020). Currently, alum with high safety is the only adjuvant approved by the Food and Drug Administration (FDA) for human vaccines. However, alum also has some disadvantages, such as anergy to cellular immunity and poor immunogenicity (Kool et al., 2012). Therefore, it is urgent to develop new vaccine adjuvants with great potency but much lower toxicity.

With the development of nanotechnology, nanoparticles as vaccine adjuvants have gained widespread attention because nanoparticles can protect the protein antigen against degradation, ensure sustained antigen release, and enhance the immune response (Liu et al., 2020; Wang et al., 2020). Various nanoparticles such as polymer nanoparticles (Liu et al., 2016), liposomes (Yaghob et al., 2020), inorganic nanoparticles (Krystina et al., 2019), and gold nanoparticles (Zhang et al., 2015) have been investigated as vaccine adjuvants. Despite significant superiority, the fabrication protocol is complicated. Metal-organic frameworks (MOFs), constructed from metal ions or clusters and organic ligands via diffusion or solvothermal method, have a porous structure and ultrahigh surface area (Lawson et al., 2021). MOFs can be widely used in the field of biomedicine, such as drugs and gene delivery, biocatalysis, tissue engineering, bioimaging, cancer treatment, biosensors, and so on. (Li et al., 2019; Gumilar et al., 2020; Liu et al., 2020; Li et al., 2021; Meng et al., 2021; Niu et al., 2021; Liu et al., 2022). In recent years, protein encapsulated MOFs have been prepared as vaccine adjuvants. Sun's group had synthesized aluminum-integrated nano-MOF to deliver antigen. This delivery system enhanced antigen cross-presentation and elicited strong humoral and cellular immune responses (Zhong et al., 2019). Qu et al. developed a novel kind of MOF-based subunit vaccines. ZIF-

CONTACT Lu Wang  luwangbest@163.com  College of Animal & Veterinary Sciences, Southwest Minzu University, Chengdu, China; Tao Dai  tdaicat@163.com  College of Chemistry & Environment, Southwest Minzu University, Chengdu, China

*These authors have contributed equally to this work.

 Supplemental data for this article can be accessed [here](#).

© 2021 The Author(s). Published by Informa UK Limited, trading as Taylor & Francis Group.

This is an Open Access article distributed under the terms of the Creative Commons Attribution-NonCommercial License (<http://creativecommons.org/licenses/by-nc/4.0/>), which permits unrestricted non-commercial use, distribution, and reproduction in any medium, provided the original work is properly cited.

8 nanoparticles were used to encapsulate antigens and could adsorb the CpG ODNs through strong electrostatic interaction. The MOF-based vaccines could enhance systemic immune response and induce potent immune memory response (Zhang et al., 2016). Xue's group used MOF nanoparticles as an antigen delivery system for cotransporting the antigen model ovalbumin (OVA) and CpG. The results showed that the MOF nanoparticles could not only improve the uptake of OVA by the antigen-presenting cells but also deliver both OVA and CpG into the same cell. The delivery system induced strong cellular immunity, CTL response, and potent immune memory response (Yang et al., 2018). The MOF nanoparticles mentioned above were used to develop vaccines against cancers. Meanwhile, the fabrication of these MOF nanoparticles involved heavy metal ions, non-pharmaceutical grade organic linkers, and organic solvents, increasing production costs and causing sustained toxic effects. Thus, these MOF nanoparticles were not suitable for vaccines. The demand for a novel kind of MOFs as vaccine adjuvants is increasing.

γ -Cyclodextrin (γ -CD), a kind of cyclic oligosaccharide, is obtained from starch on the kilogram scale via microbiology degradation (Xu et al., 2021). Stoddart built a cyclodextrin metal-organic framework by combining γ -cyclodextrin with alkali metal ions, called γ -CD-MOFs. γ -CD-MOFs possessed high porosity, good biocompatibility, and a simple and green preparation process (Forgan et al., 2012). However, the adjuvanticity of γ -CD-MOFs has not been explored. Therefore, γ -CD-MOFs have broad prospects in the application of animal vaccine adjuvants.

Herein, we designed a novel kind of vaccine adjuvants (SP- γ -CD-MOF) to delivery antigen by modifying γ -CD-MOF with span-85, which was obtained in a very mild, simple and green-friendly way. The SP- γ -CD-MOF loaded with the model antigen OVA(SP- γ -CD-MOF/OVA) had the potential to enhance immune response, due to it could be sustained released of model antigen OVA and be ability to protect antigen against degradation. Furthermore, the SP- γ -CD-MOF displayed perfect biocompatibility in vivo and in vitro. More importantly, SP- γ -CD-MOF/OVA was favorable for promoting the production of OVA-specific antibodies, inducing the proliferation of spleen cells and increasing the cytokine secretion of splenocytes. In addition, SP- γ -CD-MOF/OVA induces BMDC activation and maturation and facilitates the activation of lymphocyte cells (CD4⁺ T and CD8⁺ T lymphocytes cells) to induce strong immune responses. This study highlights the SP- γ -CD-MOF/OVA complex have the potential to serve as efficient vaccines, which would expected to broaden the understanding of SP- γ -CD-MOF and its application as a vaccine adjuvant.

2. Materials and methods

2.1. Materials and instrumentation

Potassium hydroxide (KOH), methanol (MeOH), dichloromethane (CH₂Cl₂), Span 85 (SP85), and isopropanol (C₃H₈O) were purchased from Chengdu Kelong Chemical Engineering Company (Chengdu, China). γ -Cyclodextrin (γ -CD) was

purchased from Aladdin (Shanghai, China). RPMI 1640 medium, fetal bovine serum, and penicillin-streptomycin were obtained from Gibco (Carlsbad, CA, USA). Horseradish peroxidase (HRP)-conjugated goat anti-mouse IgG antibodies were obtained from Abcam Ltd (Hong Kong). GM-CSF and IL-4 were produced from Novoprotein(Suzhou, China). ELISA kits were ordered from Enzyme-Linked Biosystems (Shanghai, China). CCK-8 kit was purchased from BOSTER Biological Technology (USA).

Scanning electron microscope (SEM) was measured with JEOL-JSM-7500. X-Ray powder diffraction (XRD) was collected using Bruker D8 advance. The UV/Vis and fluorescence spectra results were detected using Varioskan LUX. Fourier transform infrared (FTIR) spectra were recorded by American Nicolet 67.

2.2. Animals

Healthy female Kunming mice (6-8 weeks) were obtained from the Chengdu Dossy Experimental Animals Co. LTD (Chengdu, China), and all animal experiments were approved by the Institutional Animal Care and Ethics Committee of Southwest Minzu University.

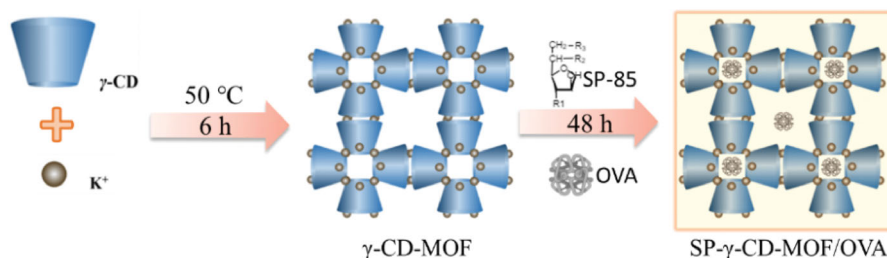
2.3. Synthesis of SP- γ -CD-MOF

γ -CD (648 mg) and KOH (224 mg) were dissolved into a 21 mL mixture solution of pure water and methanol (v/v:20:1). MeOH was allowed to vapor diffuse into the solution. After 6 h, the supernatant was transferred into MeOH with the addition of CTAB, and the solution was incubated 3 h at room temperature. The white cubic crystals were isolated, filtered, and washed with isopropanol three times. The wet sample was then dried in a vacuum oven at 45 °C for 12 h (Li et al., 2017). The white powders were collected and named γ -CD-MOF. In order to improve the stability, 100 mg γ -CD-MOF were dispersed into dichloromethane with span-85 for 48 h. Then the precipitates were collected via centrifuge at 8000 rpm for 5 minutes and washed 2–3 times with dichloromethane. The collected powders were SP- γ -CD-MOF.

The SP- γ -CD-MOF loaded with OVA(SP- γ -CD-MOF/OVA) was obtained through the same methods. The PVP-modified OVA was first prepared by adding OVA into a water solution containing PVP to stabilize OVA in the methanol solution (Zhang et al., 2016). And the synthesis process of SP- γ -CD-MOF/OVA was shown in Scheme 1.

2.4. Hemocompatibility evaluation

Firstly, the hemolysis test was performed in the blood of different animals (such as chicken, cat, dog, and rabbit). Different concentrations of SP- γ -CD-MOF suspension (1 mL) were added into red blood cell suspension (50 μ L, 16%). Ultrapure water and PBS buffer were the positive and negative groups, respectively. The solution was incubated at 37 °C for 12 h, and the supernatant was collected by centrifuge at 3000 rpm for 5 min. The absorbance of the supernatant was measured at 570 nm.



Scheme 1. The synthesis process of SP- γ -CD-MOF/OVA.

Secondly, Thrombin time (TT) was analyzed. Plasma was collected and added into SP- γ -CD-MOF suspension ($V/V=9:1$). The mixture solution was incubated for 15 min at 37 °C. After adding the TT reagent ($V/V=1:1$), the plasma clotting time was recorded. The prothrombin time (PT) was detected with the same method.

2.5. Cytotoxicity analysis of the SP- γ -CD-MOF

Cytotoxicity of SP- γ -CD-MOF for RAW246.7 cells was evaluated by the CCK-8 Kit. Firstly, RAW246.7 cells were plated at the density of 1×10^4 cells per well in 96-well plates and cultured in a cell incubator containing 5% CO₂ at 37 °C for 12 h. Then SP- γ -CD-MOF at concentrations from 0 to 100 $\mu\text{g}/\text{mL}$ was added to wells, and then cells were incubated for another 12 h. After that, 10 μL CCK-8 solution was added to each well, followed by 4 h incubation. Absorption was measured at 450 nm. Cell viability was calculated according to the equation below (Li et al., 2017):

$$\text{Cell viability (\%)} = (\text{OD sample}/\text{OD control}) \times 100\%$$

where OD control was obtained in the absence of SP- γ -CD-MOF.

2.6. Immunization of mice

The mice were randomly divided into four groups with five mice in each group and immunized with 100 μL of SP- γ -CD-MOF/OVA, SP- γ -CD-MOF, and free OVA via subcutaneous injection. The control group was injected with 100 μL PBS. The mice were immunized 3 times on days 0, 14, 28, and sera were collected on days 7, 21, 35. On the 14th day after the third immunization, all of the mice were sacrificed to collect splenocytes.

2.7. Elisa determination of OVA-specific antibodies in serum

The OVA-specific antibody levels were determined according to the previous report (Jia et al., 2017). In brief, ELISA 96-well plates were coated with 100 μL of OVA per well (2 $\mu\text{g}/\text{mL}$) in coating buffer (50 mM Na₂CO₃-NaHCO₃, pH 9.6) and incubated overnight at 4 °C. Then, the plates were washed with PBST (0.05% Tween 20 in PBS) and blocked with 200 μL 1% BSA in PBST for 1 h at 37 °C. After washing with PBST four times, sera dilutions were added to the plates, and the plates were incubated for 1 h at 37 °C. The plates were stained with

the antibody of Anti-Mouse and incubated for 40 min. The plates were again incubated with TMB substrate for 20 min in the dark. H₂SO₄ was added to stop the enzymatic reaction. At last, the adsorption values were measured at 450 nm. The titers of IgG were determined as the maximum dilution that the absorbance value was twice higher than that of negative serum.

2.8. Splenocyte proliferation assay

Spleens were collected from the immunized mice, and the splenocyte suspension was obtained via grinding through a cell strainer and splitting the erythrocytes. Then, the splenocytes were seeded in the plate with 5×10^6 cells/mL and incubated with OVA, SP- γ -CD-MOF, SP- γ -CD-MOF/OVA, or nothing for 72 h. Thereafter, each well was added 10 μL CCK-8 solution and incubated for another 4 h. Finally, the absorbance was evaluated at 450 nm. The proliferation index (PI) was calculated according to the following equation (Yang et al., 2018): $\text{PI} = \text{OD}_{450}$ for stimulated cultures/ OD_{450} for non-stimulated cultures.

2.9. Cytokine expression of splenocytes in vitro

Splenocytes were cultured with RPMI 1640 and treated with OVA (30 $\mu\text{g}/\text{mL}$). After incubation for 72 h, the supernatants were harvested. The levels of TNF- α , IFN- γ and IL-4 in supernatants were measured using ELISA Kits.

2.10. Detection of CD4⁺ and CD8⁺ T cells

Splenocytes were re-stimulated with OVA (30 $\mu\text{g}/\text{mL}$) for 72 h at 37 °C. Then the cells were stained with fluorescent-labeled antibodies against CD4, CD8. The percentages of CD4⁺, CD8⁺ was analyzed by flow cytometry (Jia et al., 2017).

2.11. Evaluation of the maturation of bone marrow-derived dendritic cells (BMDCs)

Briefly, BMDCs were harvested from the femur and tibia and incubated with GM-CSF and IL-4 (10 and 50 ng/mL, respectively) for 6 days. Then, the BMDCs were cultured with OVA, SP- γ -CD-MOF, SP- γ -CD-MOF/OVA, or nothing for 24 h. The cytokines (IL-6, IL-1 β) of supernatant were quantified using ELISA kits.

2.12. Histopathology assay

The liver and kidney of the mice were obtained after immunization. Tissue slices were prepared by hematoxylin and eosin (H&E) and the histopathological changes were observed via a microscope.

3. Results and discussion

3.1. Characterization of SP- γ -CD-MOF particles

In this study, the vaccine adjuvant of SP- γ -CD-MOF was prepared via solvent evaporation, with a uniform diameter of about 1 μm (Figure 1(A)). After mixing OVA with SP- γ -CD-MOF, SP- γ -CD-MOF/OVA was obtained. For comparison, the pure γ -CD-MOF was also synthesized. According to the scanning electron microscopy (SEM) images (Figure 1(B)), the morphology and size of SP- γ -CD-MOF and SP- γ -CD-MOF/OVA were similar to γ -CD-MOF (Figure 1(C,D)). To further confirm the structure, Fourier transform infrared (FTIR) spectra was measured. As can be seen in Figure 2(A), the spectrum of SP- γ -CD-MOF appeared C=C stretching vibrations of Span 85 at 1560.15 cm^{-1} , which indicated that Span 85 was modified on the surface of γ -CD-MOF. And the spectrum of SP- γ -CD-

MOF/OVA exhibited stretching vibrations of C=O (1658.03 cm^{-1}) and -NH (3471.30 cm^{-1}), which appeared in the spectrum of OVA. Thus, SP- γ -CD-MOF/OVA was successfully synthesized. The amount of loaded OVA was quantified with the bicinchoninic acid assay (BCA) (Figure S2), and 6 μg OVA could be loaded onto MOF nanoparticles per milligrams. The X-ray diffraction (XRD) pattern of SP- γ -CD-MOF, SP- γ -CD-MOF/OVA and pure γ -CD-MOF were also measured and no significant difference was found. (Figure 2). The results suggested that the loaded OVA did not affect the crystal structure and particle size of SP- γ -CD-MOF.

3.2. The biocompatibility assessment in vitro and in vivo

Red blood cell hemolysis is a common indicator of biosafety. Higher hemolysis activity for red blood cells indicates lower biological safety (Zhang et al., 2016). In the study, five species were chosen to assess the hemolysis activity of SP- γ -CD-MOF at the concentration of 0.1–10 mg/mL (Figure 3(A)). SP- γ -CD-MOF displayed no hemolytic activity to chickens, mice, and goats at high or low concentrations for 12 h incubation. In rabbit red blood cells, effective hemolysis was perceived, and the hemolysis rate of SP- γ -CD-MOF was raised

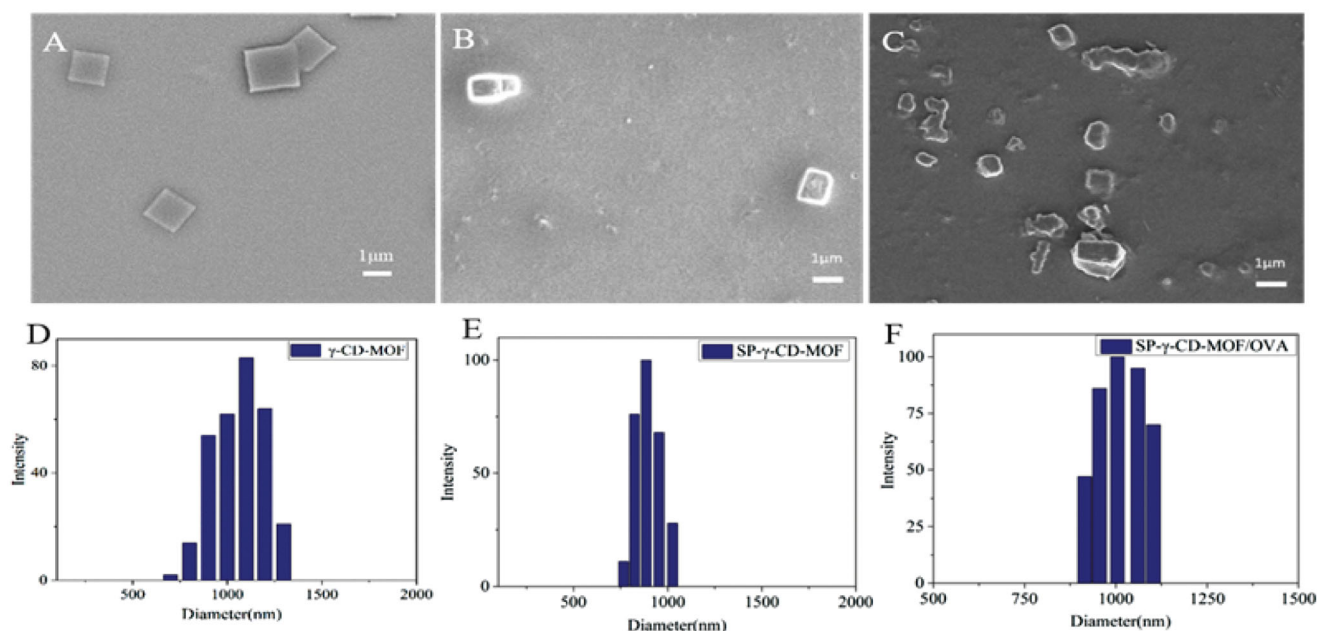


Figure 1. The SEM images of γ -CD-MOF (A), SP- γ -CD-MOF (B) and SP- γ -CD-MOF/OVA (C). The DLS pattern of γ -CD-MOF (D), SP- γ -CD-MOF (E) and SP- γ -CD-MOF/OVA (F).

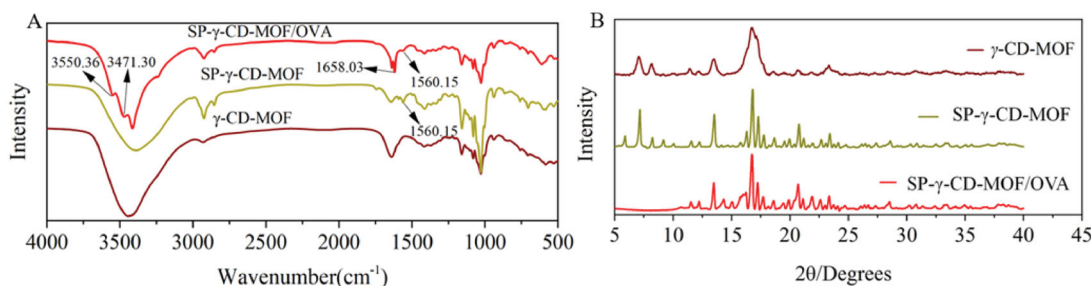


Figure 2. The FTIR spectra (A) and XRD pattern (B) of γ -CD-MOF, SP- γ -CD-MOF and SP- γ -CD-MOF/OVA.

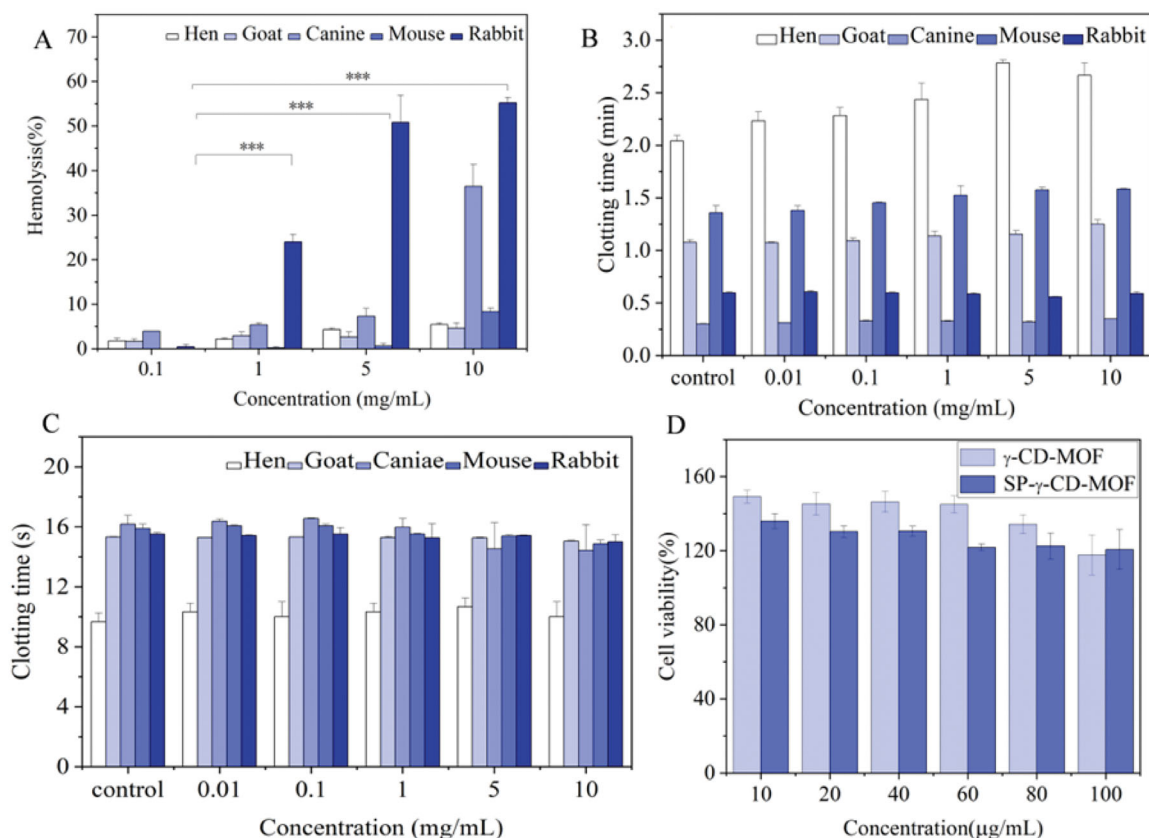


Figure 3. (A) The red blood cell hemolysis results of γ -CD-MOF and SP- γ -CD-MOF. (B) Thrombin time of γ -CD-MOF and SP- γ -CD-MOF in different species of animals. (C) Prothrombin time of γ -CD-MOF and SP- γ -CD-MOF. (D) The cytotoxicity assessment results of γ -CD-MOF and SP- γ -CD-MOF. (***) $p < .001$.

significantly with the increase of concentration. The results showed significant differences in hemolytic activity among different species. In addition, the hemolysis rate of dog red blood cells was negligible in the concentration range (0.1–5 mg/mL). When the concentration increased to 10 mg/mL, the hemolytic rate was 35%. Therefore, SP- γ -CD-MOF had excellent biosafety for kinds of animals *in vivo*.

Thrombin time (TT) and prothrombin time (PT), representing intrinsic coagulation and exogenous coagulation time, respectively, were used to evaluate plasma coagulation and reflect biocompatibility. As shown in Figure 3(B,C), TT and PT values for five species of animals are positively correlated with the concentration of SP- γ -CD-MOF, in contrast with no significant differences in the control group are observed. Thus, SP- γ -CD-MOF cannot affect TT and PT. The results further confirmed that SP- γ -CD-MOF had good blood compatibility.

For the safety of SP- γ -CD-MOF prior to animal investigations, the cytotoxicity of SP- γ -CD-MOF was assessed on RAW246.7 cells by CCK-8 (Figure 3(D)). The results revealed that SP- γ -CD-MOF had extremely high cell viability until the concentration reached 100 μ g/mL. In addition, the histopathological was studied to estimate the cytotoxicity *in vivo*. The images of organ slices (liver, kidney injected with SP- γ -CD-MOF and SP- γ -CD-MOF/OVA) show no recognizable morphologic abnormalities (Figure 4). All indicators of the blood treated with SP- γ -CD-MOF and SP- γ -CD-MOF/OVA were in the normal range (Table S1). The above results demonstrated that SP- γ -CD-MOF exhibited perfect

biocompatibility and biosafety. Thus, SP- γ -CD-MOF could be used as vaccine adjuvants to deliver antigen.

3.3. Evaluations of OVA-specific immune response

In addition to good biocompatibility, preminent adjuvants should also enhance immunity. Thus, we investigated the ability of the SP- γ -CD-MOF to induce OVA-specific humoral immunity *in vivo*. The OVA-specific IgG titers for immunized mice were measured by ELISA (Figure 5(A)). The IgG titers immunized with SP- γ -CD-MOF/OVA are higher than that immunized with free OVA, while there is no significant difference for IgG titers between SP- γ -CD-MOF/OVA and Freund's adjuvant antigen (FCA/OVA) (Figure S3). The results indicated that the SP- γ -CD-MOF had the same strength as Freund's adjuvant to enhance immune response. Furthermore, splenocyte proliferation efficiency could indirectly reflect the immune effect. The splenocyte proliferation assay was conducted with a CCK-8 kit after stimulation with SP- γ -CD-MOF/OVA for 72 h, to evaluate the efficacy of activating splenocytes. In Figure 5(B), the PIs of SP- γ -CD-MOF/OVA, OVA, and FCA/OVA are 1.39, 0.65, and 1.13, respectively. The splenocyte cells treated with SP- γ -CD-MOF/OVA proliferated more efficiently than other groups. Thus, the SP- γ -CD-MOF/OVA could enhance splenocyte proliferation more significantly and induce an OVA-specific immune response to prevent the intrusion of antigens. Therefore, SP- γ -CD-MOF is an excellent immune adjuvant for animals, with perfect biocompatibility and immune-enhancing effects.

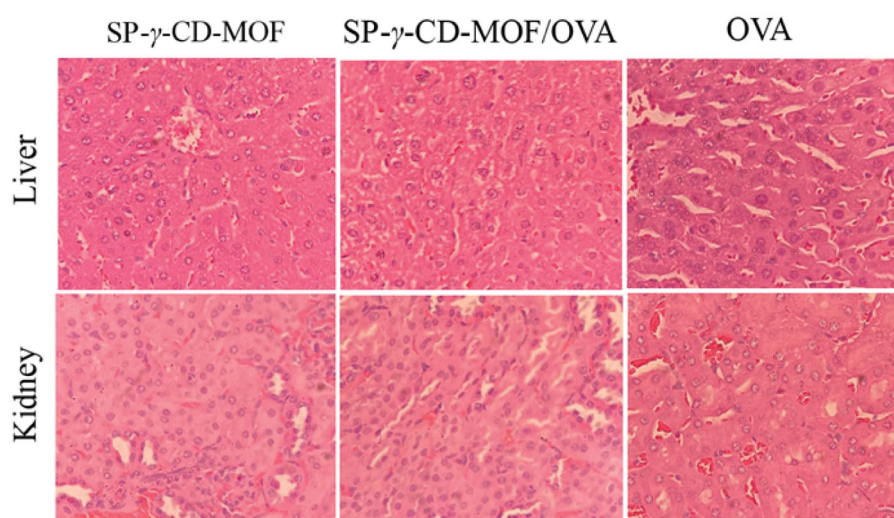


Figure 4. Hematoxylin and eosin (H&E) staining of histological sections ($\times 100$) (liver, kidney).

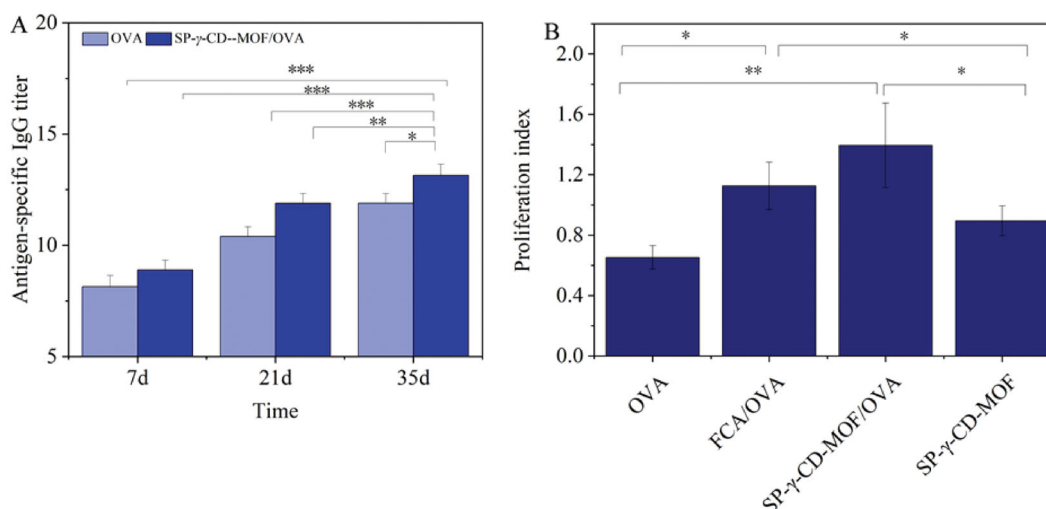


Figure 5. (A) The antigen-specific titers of IgG at indicated time points. (B) Splenocyte proliferation index. (* $p < .05$, ** $p < .01$, *** $p < .001$).

3.4. Analysis of cytokine secretion levels

The cytokine secretion levels reflect the effect of immune responses. In order to further evaluate the adjuvanticity of SP- γ -CD-MOF, the levels of Th1-type IFN- γ , TNF- α , and Th2-type IL-4 from splenocytes were measured by ELISA. According to Figure 6(A,B), the concentrations of IFN- γ and TNF- α cytokines production by SP- γ -CD-MOF/OVA are higher than free OVA and FCA/OVA, indicating that SP- γ -CD-MOF/OVA can improve the IFN- γ and TNF- α secretion by splenocytes. While the levels of IFN- γ and TNF- α treated with FCA/OVA and SP- γ -CD-MOF/OVA are not significantly different. IFN- γ played an important role in the differentiation of Th0 cells to Th1 cells and the promotion of T cell responses. TNF- α could regulate adaptive immunity. Both IFN- γ and TNF- α were representative cytokines of cellular immune responses. Thereby, the results revealed that SP- γ -CD-MOF/OVA enhanced cellular immunity. In addition, the IL-4, a Th2-type cytokine, is shown in Figure 6(C). The IL-4 level in SP- γ -CD-MOF/OVA group is slightly higher than that in the OVA, but not different, compared with OVA and SP- γ -CD-MOF/OVA. In

all, SP- γ -CD-MOF/OVA induced higher secretion of Th1 and Th2 cytokines by splenocytes improving immune responses.

3.5. BMDCs activation and maturation in vitro

The mature DCs played a vital role in antigen presentation and immune response induction. High expression of cytokines was the sign of DC maturation. In order to evaluate the adjuvanticity of SP- γ -CD-MOF, the secreted cytokines by BMDCs, including IL-1 β , IL-12, IL-4, and IL-6, were evaluated using ELISA kit. As shown in Figure 7, SP- γ -CD-MOF/OVA induces the greater production of inflammatory cytokines IL-1 β between OVA and SP- γ -CD-MOF/OVA. Meanwhile, Th1-polarizing cytokines IL-12 induces protective immune responses. The level of IL-12 treatment with SP- γ -CD-MOF/OVA is remarkably higher in comparison with OVA, indicating that SP- γ -CD-MOF/OVA can enhance BMDC maturation. Besides, SP- γ -CD-MOF/OVA treatment efficiently promotes the secretion of IL-6 and IL-4. Hence, the results confirmed that SP- γ -CD-MOF/OVA could activate and mature BMDCs,

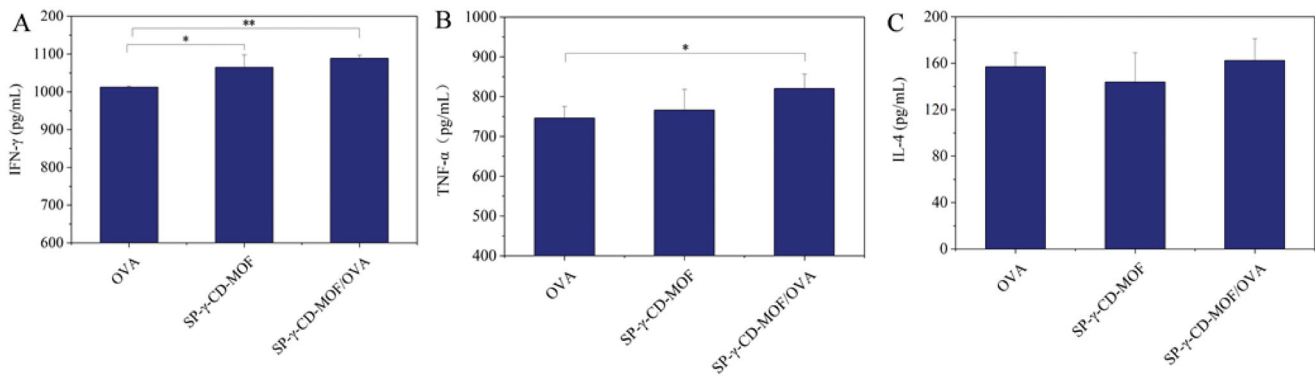


Figure 6. The levels of cytokine secretion by splenocytes. IFN- γ (A), TNF- α (B), and IL-6 (C). (* $p < .05$, ** $p < .01$).

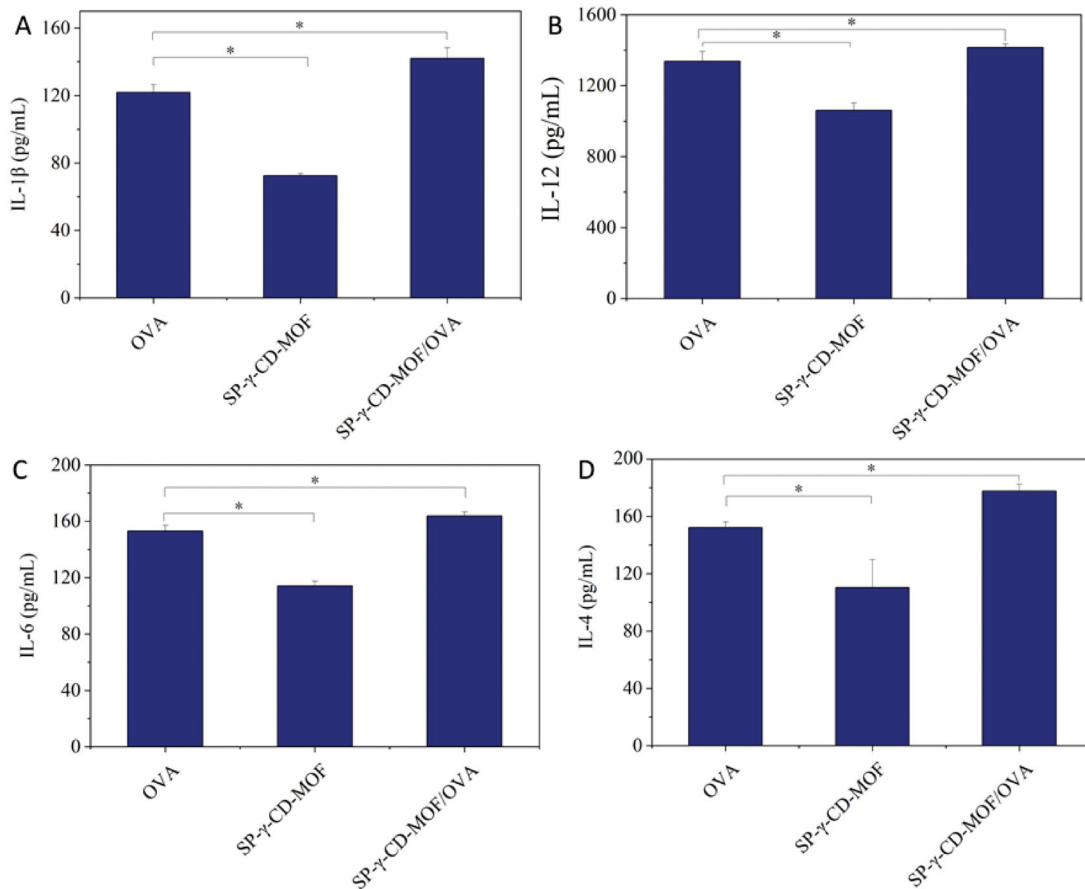


Figure 7. Cytokine release of BMDCs stimulated with various adjuvants. (A) IL-1 β , (B) IL-12, (C) IL-6, and (D) IL-4. (* $p < .05$).

enhance antigen processing, and induce protective immune responses.

3.6. Lymphocyte activation

T cells, as important lymphocytes, mediate immunity. CD8⁺ T cells can recognize endogenous antigens, while CD4⁺ T cells play an important role in the activation and regulation of specific immune responses. The proportion of CD8⁺ T and CD4⁺ T cells reflected the strength of the immune response. CD4⁺ T and CD8⁺ T cells of splenocytes were measured with labeling specific antibodies. The results showed that the percentage of CD4⁺ T and CD8⁺ T cells from SP- γ -CD-MOF/OVA was 0.98%. And in the OVA group, the percentage of CD4⁺ T

and CD8⁺ T cells was only 0.54% (Figure 8). SP- γ -CD-MOF/OVA significantly increased the proportion of CD4⁺ T and CD8⁺ T cells more than other groups. The activation of immune cells initiated the whole immune response. The effective activation of effector lymphocyte cells initiated the immune reaction and induced effective specific immune responses.

4. Conclusions

In this study, we developed a kind of SP- γ -CD-MOF with simplicity, convenience, and greenness, through solvent evaporation. In terms of biocompatibility and cost-effectiveness, SP- γ -CD-MOF as vaccine adjuvant was evaluated. The SP- γ -

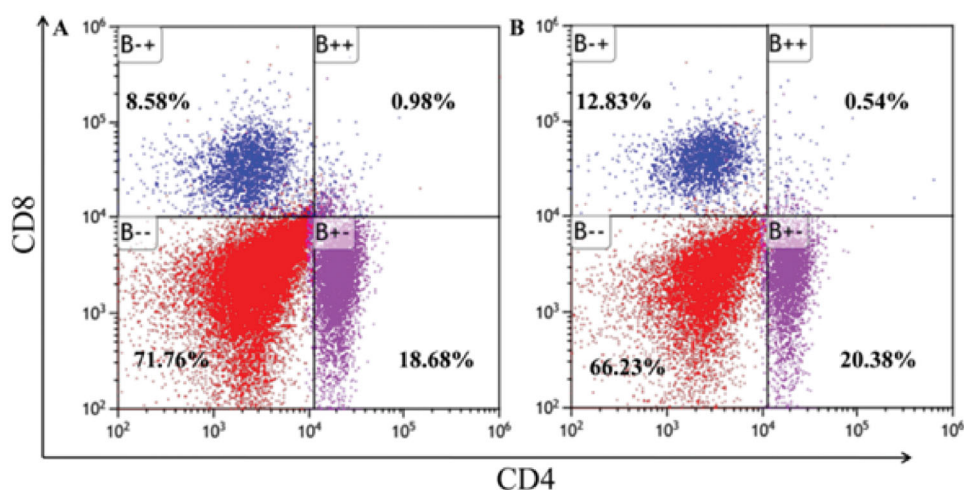


Figure 8. Graph of frequency of CD4⁺ and CD8⁺ T cells. (A) OVA (B)SP- γ -CD-MOF/OVA.

CD-MOF loaded with OVA (SP- γ -CD-MOF/OVA) can promote the production of OVA-specific antibodies, enhance splenocyte proliferation, and increase the cytokine secretion of splenocytes. In addition, SP- γ -CD-MOF/OVA induces BMDC activation and maturation and facilitates the activation of lymphocyte cells (CD4⁺ T and CD8⁺ T lymphocytes cells) to induce strong immune responses. This study shows the potential of SP- γ -CD-MOF in vaccine adjuvants and provides a novel idea for the development of vaccine adjuvants. We envision that the SP- γ -CD-MOF could be possible used to deliver mRNA, DNA and other specific antigen against bacterial and virus infections. Beyond this, this finding lays the foundation for the design of other safe and effective vaccine adjuvants, which would facilitate the application in biomedical areas.

Disclosure statement

No potential conflict of interest was reported by the author(s).

Funding

This work was financially supported by National Science Foundation of China [21908183], Science and Technology Innovation and Entrepreneurship Seedling Key Projects of Sichuan Province [22MZGC0294] and Innovative Research Projects for Postgraduate Students, Southwest Minzu University [CX2020SZ50].

ORCID

Tao Dai  <http://orcid.org/0000-0002-6702-888X>

References

- Baldwin MR, Tepp WH, Przedpelski A, et al. (2008). Subunit vaccine against the seven serotypes of botulism. *Infect Immun* 76:1314–8.
- Bobbala S, Hook S. (2016). Is there an optimal formulation and delivery strategy for subunit vaccines. *Pharm Res* 33:2078–97.
- Forgan RS, Smaldone RA, Gassensmith JJ, et al. (2012). Nanoporous carbohydrate metal-organic frameworks. *J Am Chem Soc* 134:406–17.
- Gumilar G, Kaneti YV, Henzie J, et al. (2020). General synthesis of hierarchical sheet/plate-like M-BDC (M=Cu, Mn, Ni, and Zr) metal-organic frameworks for electrochemical non-enzymatic glucose sensing. *Chem Sci* 11:3644–55.
- Jia JL, Liu Q, Yang TY, et al. (2017). Facile fabrication of varisized calcium carbonate microspheres as vaccine adjuvants. *J Mater Chem B* 5: 1611–23.
- Kool M, Fierens K, Lambrecht BN. (2012). Alum adjuvant: some of the tricks of the oldest adjuvant. *J Med Microbiol* 61:927–34.
- Krystina L, Hess L, Jewell M. (2019). Designing inorganic nanomaterials for vaccines and immunotherapies. *Nano Today* 27:73–98.
- Lawson HD, Walton SP, Chan C. (2021). Metal-organic frameworks for drug delivery: a design perspective. *ACS Appl Mater Interfaces* 13: 7004–20.
- Li F, Chun Z, Qi S, et al. (2019). Efficacy of CPG-ODN and Freund's immune adjuvants on antibody responses induced by chicken infectious anemia virus Vp1, Vp2, and Vp3 subunit proteins. *Poult Sci* 98: 1121–6.
- Li HY, Lv NN, Li X, et al. (2017). Composite CD-MOF nanocrystals-containing microspheres for sustained drug delivery. *Nanoscale* 9: 7454–63.
- Li JJ, Xia W, Tang J, et al. (2019). MOF nanoleaves as new sacrificial templates for the fabrication of nanoporous Co-Nx/C electrocatalysts for oxygen reduction. *Nanoscale Horiz* 4:1006–13.
- Li M, Liu Y, Li F, et al. (2021). Defect-rich hierarchical porous uio-66(zr) for tunable phosphate removal. *Environ Sci Technol* 55:13209–18.
- Li Y, Li M, Gong T, et al. (2017). Antigen-loaded polymeric hybrid micelles elicit strong mucosal and systemic immune responses after intranasal administration. *J Control Release* 262:151–8.
- Liu B, Jiang M, Zhu DZ, et al. (2022). Metal-organic frameworks functionalized with nucleic acids and amino acids for structure- and function-specific applications: a tutorial review. *Chem Eng J* 428: 131118.
- Liu JD, Wang ZK, Bi R, et al. (2020). A polythreaded MnII-MOF and its super-performances for dye adsorption and supercapacitors. *Inorg Chem Front* 7:718–30.
- Liu JJ, Miao L, Sui JY, et al. (2020). Nanoparticle cancer vaccines: design considerations and recent advances. *Asian J Pharm Sci* 15:576–90.
- Liu Q, Jia JL, Yang TY, et al. (2016). Pathogen-mimicking polymeric nanoparticles based on dopamine polymerization as vaccines adjuvants induce robust humoral and cellular immune responses. *Small* 12: 1744–57.
- Lukacs M, Haanes KA, Majlath Z, et al. (2015). Dural administration of inflammatory soup or complete Freund's adjuvant induces activation and inflammatory response in the rat trigeminal ganglion. *J Headache Pain* 16:564–74.

- Meng L, Zhang L, Zhu Y, et al. (2021). Highly dispersed secondary building unit-stabilized binary metal center on a hierarchical porous carbon matrix for enhanced oxygen evolution reaction. *Nanoscale* 13: 1213–9.
- Nakamura Y, Fukushige R, Watanabe K, et al. (2020). Continuous infusion of substance P inhibits acute, but not subacute, inflammatory pain induced by complete Freund's adjuvant. *Biochem Biophys Res Commun* 533:971–5.
- Niu Z, Cui X, Pham T, et al. (2021). A MOF-based ultra-strong acetylene nano-trap for highly efficient C₂ H₂/CO₂ separation. *Angew Chem Int Ed Engl* 60:5283–8.
- Wang WJ, Zhou XX, Bian YJ, et al. (2020). Dual-targeting nanoparticle vaccine elicits a therapeutic antibody response against chronic hepatitis B. *Nat Nanotechnol* 15:406–16.
- Xu WJ, Li XM, Wang L, et al. (2021). Design of cyclodextrin-based functional systems for biomedical applications. *Front Chem* 9:635507.
- Yaghob A, Ehsan A, Amirhossein A. (2020). Targeting strategies in therapeutic applications of toxoplasmosis: recent advances in liposomal vaccine delivery systems. *Current Drug Targets* 21:541–58.
- Yang Y, Chen QQ, Wu JP, et al. (2018). Reduction-responsive codelivery system based on a metal-organic framework for eliciting potent cellular immune response. *ACS Appl Mater Interfaces* 10:12463–73.
- Zhang PP, Chiu YC, Tostanoski LH, Jewell CM. (2015). Polyelectrolyte multilayers assembled entirely from immune signals on gold nanoparticle templates promote antigen-specific T cell response. *ACS Nano* 9: 6465–77.
- Zhang Y, Cai J, Li C, et al. (2016). Effects of thermosensitive poly(N-isopropylacrylamide) on blood coagulation. *J Mater Chem B* 4:3733–49.
- Zhang Y, Wang FM, Ju EG, et al. (2016). Metal-organic-framework-based vaccine platforms for enhanced systemic immune and memory response. *Adv Funct Mater* 26:6454–61.
- Zhao Z, Zhang C, Lin Q, et al. (2020). Single-walled carbon nanotubes as delivery vehicles enhance the immunoprotective effect of an immersion DNA vaccine against infectious spleen and kidney necrosis virus in Mandarin Fish. *Fish Shellfish Immunol* 97:432–9.
- Zhong XF, Zhang YT, Tan L, et al. (2019). An aluminum adjuvant-integrated nano-MOF as antigen delivery system to induce strong humoral and cellular immune responses. *J Control Release* 300:81–92.